NASA/TM-20240012991

Spectrally Efficient GaN High-Power Amplifier for Lunar Communications

Rainee N. Simons, Marie T. Piasecki, Joseph A. Downey, and Bryan L. Schoenholz
Glenn Research Center, Cleveland, Ohio

November 2024

NASA STI Program Report Series

Since its founding, NASA has been dedicated to the advancement of aeronautics and space science. The NASA scientific and technical information (STI) program plays a key part in helping NASA maintain this important role.

The NASA STI program operates under the auspices of the Agency Chief Information Officer. It collects, organizes, provides for archiving, and disseminates NASA's STI. The NASA STI program provides access to the NTRS Registered and its public interface, the NASA Technical Reports Server, thus providing one of the largest collections of aeronautical and space science STI in the world. Results are published in both non-NASA channels and by NASA in the NASA STI Report Series, which includes the following report types:

- TECHNICAL PUBLICATION. Reports of completed research or a major significant phase of research that present the results of NASA programs and include extensive data or theoretical analysis. Includes compilations of significant scientific and technical data and information deemed to be of continuing reference value. NASA counterpart of peer-reviewed formal professional papers but has less stringent limitations on manuscript length and extent of graphic presentations.

- TECHNICAL MEMORANDUM. Scientific and technical findings that are preliminary or of specialized interest, e.g., quick release reports, working papers, and bibliographies that contain minimal annotation. Does not contain extensive analysis.

- CONTRACTOR REPORT. Scientific and technical findings by NASA-sponsored contractors and grantees.

- CONFERENCE PUBLICATION. Collected papers from scientific and technical conferences, symposia, seminars, or other meetings sponsored or cosponsored by NASA.

- SPECIAL PUBLICATION. Scientific, technical, or historical information from NASA programs, projects, and missions, often concerned with subjects having substantial public interest.

- TECHNICAL TRANSLATION. English-language translations of foreign scientific and technical material pertinent to NASA's mission.

Specialized services also include organizing and publishing research results, distributing specialized research announcements and feeds, providing information desk and personal search support, and enabling data exchange services.

For more information about the NASA STI program, see the following:

- Access the NASA STI program home page at http://www.sti.nasa.gov

NASA/TM-20240012991

Spectrally Efficient GaN High-Power Amplifier for Lunar Communications

Rainee N. Simons, Marie T. Piasecki, Joseph A. Downey, and Bryan L. Schoenholz
Glenn Research Center, Cleveland, Ohio

National Aeronautics and
Space Administration

Glenn Research Center
Cleveland, Ohio 44135

November 2024

Acknowledgments

The authors would like to thank Nicholas Varaljay for installing the DC bias harness on the HPAs and the Space Communications and Navigation (SCaN) Program for their support. This NASA Technical Memorandum (TM) is an expanded version of the one-page Abstract that was presented at the 2024 IEEE International Symposium on Antennas and Propagation and ITNC-USNC-URSI Radio Science Meeting at the ”Fortezza da Basso” Convention Center, Florence, Italy, July 14 to 19, 2024. The Figures for this NASA TM are archived under E-20271.

Level of Review: This material has been technically reviewed by technical management.

This report is available in electronic form at https://www.sti.nasa.gov/ and https://ntrs.nasa.gov/

NASA STI Program/Mail Stop 050
NASA Langley Research Center
Hampton, VA 23681-2199

Spectrally Efficient GaN High-Power Amplifier for Lunar Communications

Rainee N. Simons, Marie T. Piasecki, Joseph A. Downey, and Bryan L. Schoenholz
National Aeronautics and Space Administration
Glenn Research Center
Cleveland, Ohio 44135

Abstract

The paper demonstrates a spectrally efficient Ka-band GaN MMIC based high-power amplifier (HPA) that uses a waveguide 4-port magic-tee as a 2-way power combiner to combine the output from two lower power amplifier circuits. The paper presents for the prototype HPA the measured output power, gain, power added efficiency, error vector magnitude for Offset-QPSK, 8PSK, 16APSK, 32APSK, and 16QAM waveforms, waveform spectrum, and out-of-band spectral regrowth. The HPA is intended for establishing a direct communication link between assets on the lunar surface/orbit and Earth.

1.0 Introduction

Robust communications links between the assets on the lunar surface/orbit and Earth are required to ensure astronaut's health/safety while traveling to the surface of the Moon and for robotic exploration of the lunar surface. These links can additionally serve as a conduit to transfer data from science instruments placed on the lunar surface. Since signals from the lunar surface/orbit must travel large distances, high-power amplifiers (HPAs) at the output of the transmitters are required to ensure adequate signal-to-ratio (SNR) at the receivers on Earth. Typically, the output power from a single gallium nitride (GaN) high electron mobility transistor (HEMT) based monolithic microwave integrated circuit (MMIC) power amplifier (PA) chip used in building a HPA is limited to few watts and is inadequate to meet the above requirements. Hence, a power combining circuit that can combine the output power from several such PA chips to ensure that the transmitter power is adequate to overcome the path losses and meet the receiver SNR requirements is desired.

Power combining of two or more PA chips have been demonstrated by several investigators. In References 1 and 2 a 16-way waveguide based radial power splitter/combiner to combine the output from 16 GaN MMIC PAs has been demonstrated across the 17.3 to 20.2 GHz and 28 to 38 GHz frequency range, respectively. In Reference 3, the output from 4 GaN MMIC PAs are combined using a 4-way power splitter/combiner design that is based on binary, 2-tier waveguide H-plane junctions for applications across the 31 to 34 GHz frequency range.

This paper builds on our prior investigations of power combiners for combining the output from multiple high power space traveling-wave tube amplifiers (TWTAs) (Ref. 4) and (Ref. 5). Additionally, we have also carried out computer aided design of several hybrid junctions including magic-tee as elements within a corporate power combining architecture for high power TWTAs (Ref. 6). In the above references, we demonstrate the use of a waveguide based 4-port magic-tee as a 2-way power combiner to combine the output power from two 100-watt space TWTs at Ka-band frequencies (31.8 to 32.3 GHz) designated for deep space interplanetary communications.

Recently, we demonstrated a prototype of a switched wideband GaN HEMT based MMIC HPA that operates across the 25.25 to 31 GHz frequency band for user spacecraft terminals to support interoperability with multiple commercial SATCOM networks (Ref. 7). Furthermore, we investigated the benefits offered by GaN HPA's performance characteristics for user spacecraft cognitive radio platforms that can learn from the environment in which they are operating and adaptively and dynamically change the operating parameters (Ref. 8). Moreover, we demonstrated a prototype GaN HPA that operates over the 23.15 to 23.55 GHz frequency band for future lunar proximity communication forward links that are planned between assets located in the lunar orbit and lunar surface, cross links between lunar relays, and links to science mission spacecraft (Ref. 9).

In this paper, we present a prototype HPA, based on a waveguide 4-port magic-tee as a 2-way power combiner to combine the output from two GaN MMIC PA chips. The intended application is for direct-to-Earth communications from the vicinity of the Moon at the designated 27 to 27.5 GHz frequency range. In addition, the paper presents the measured output power, gain, power added efficiency (PAE), and error vector magnitude for Offset-QPSK, 8PSK, 16APSK, 32APSK, and 16QAM waveforms. Furthermore, the output spectrum and the out-of-band spectral regrowth for the Offset-QPSK and 8PSK waveforms when the HPA is operated at saturation and for the 16APSK, 32APSK, and 16QAM waveforms when the HPA is operated 1-dB backed-off from saturation are also presented.

2.0 High Power Amplifier Architecture and Brief Set of Requirements

The architecture of a 2-way power combiner based on a waveguide hybrid magic-tee is shown in Figure 1(a). In this approach, the two PAs are coupled to Ports #1 and #4 (H-Plane and the E-Plane ports along the plane of symmetry) of the magic-tee, respectively. The incident power at Port #1 (from PA #1) is evenly split into two in-phase components between Ports #2 and #3 of the magic-tee. The power incident at Port #4 (from PA #2) is also evenly split but with 180° phase difference between Ports #2 and #3 of the magic-tee. The magic-tee is designed such that the electrical lengths between any port and the junction are identical. Thus, by superposition principle, the power at Port #3 must add in phase while at Port #2 must result in perfectly cancellation. Consequently, Ports #3 and #2 are referred to as the sum and difference ports, respectively. This 2-way combiner architecture can be extended in a binary configuration to obtain very high power by combining 2^n PAs, where n is an integer as illustrated in Figure 1(b).

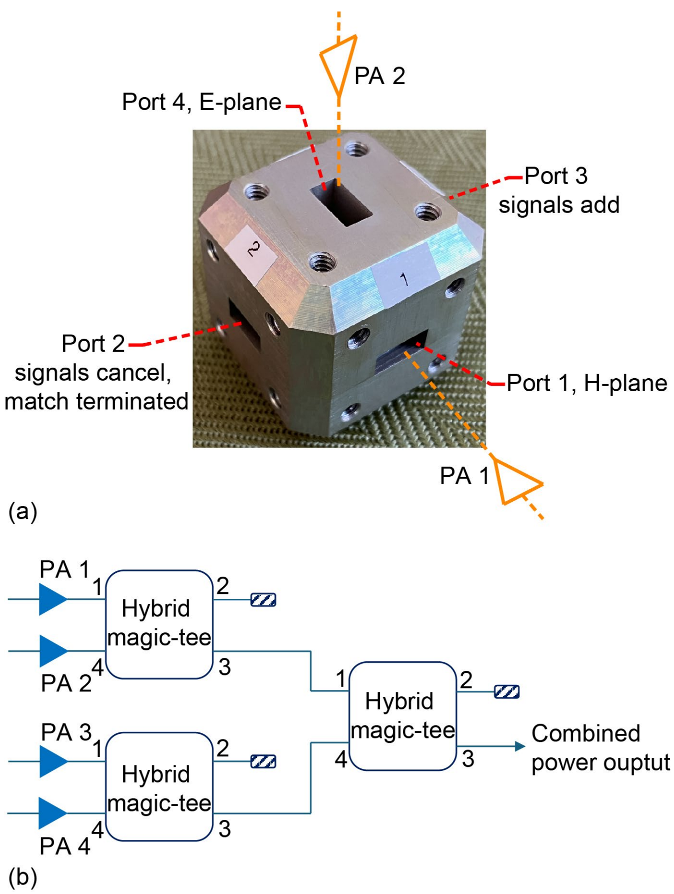

Figure 1.—(a) Waveguide (WR–28) hybrid magic-tee used in power combiner circuit, insertion loss (S_{21} and S_{31}) and (S_{24} and S_{34}) = 0.5 dB, isolation (S_{41} and S_{14}) = 30 dB, impedance match (S_{11} and S_{44}) > 10 dB. (b) Binary circuit architecture for combining 2^n PAs, where n is an integer (shown here for n = 2). PAs are Qorvo QPA2212D and magic-tee is QuinStar QJH-AL2900.

A brief set of requirements for the prototype HPA with 2-way power combiner circuit are as follows:

- Saturated output power (P_{sat}): 30 W
- Bandwidth: 27 to 27.5 GHz
- Peak PAE: 18 to 20 percent
- Small signal gain: 20 dB
- Gain flatness over full bandwidth: ± 1 dB or better
- Input/Output return Loss (dB): > 10 dB

3.0 High Power Amplifier Architecture Performance Validation

The performance of the prototype HPA is characterized using Rohde & Schwarz (R&S) SMW200A Vector Signal Generator (VSG), R&S FSW43 Signal and Spectrum Analyzer, and Keysight N6705C DC Power Analyzer. The test setup for characterizing the prototype HPA is shown in Figure 2.

3.1 Phase and Amplitude Matching of the Input Signals to the Magic-Tee Based Power Combiner Circuit

To phase match the two input signals to the magic-tee a short length of a coaxial line is included in one of the input ports as shown in Figure 3. A small difference in the two-power amplifier gate bias voltages V_{g1} and V_{g2} enables amplitude matching. At the center frequency (f_0) of 27.25 GHz, with this simple arrangement, the measured output power at Port #3 is 22.38 dB higher than the output power at Port #2 as shown in Figure 4. Thus, in the prototype HPA at f_0, the output power at Port #2 is small.

3.2 Output Power, Gain, and Power Added Efficiency

The prototype HPA using magic-tee for 2-way power combining is shown in Figure 5. The measured output power (P_{out}) at Port #3 of the magic tee and the associated gain at the carrier frequency or center frequency (f_0) of 27.25 GHz are presented in Figure 6(a). The operating drain voltages (V_{d1} and V_{d2}) and gate voltages (V_{g1} and V_{g2}) are indicated in the figure caption. The corresponding PAE is presented in Figure 6(b). At f_0, the P_{sat} is 44.83 dBm (30.41 W), small signal gain is 27.5 dB, and the peak PAE is 18.7 percent. Similar sets of results have been obtained at the lower and upper band edges frequencies of 27 and 27.5 GHz, respectively. The above results are within the specifications indicated previously.

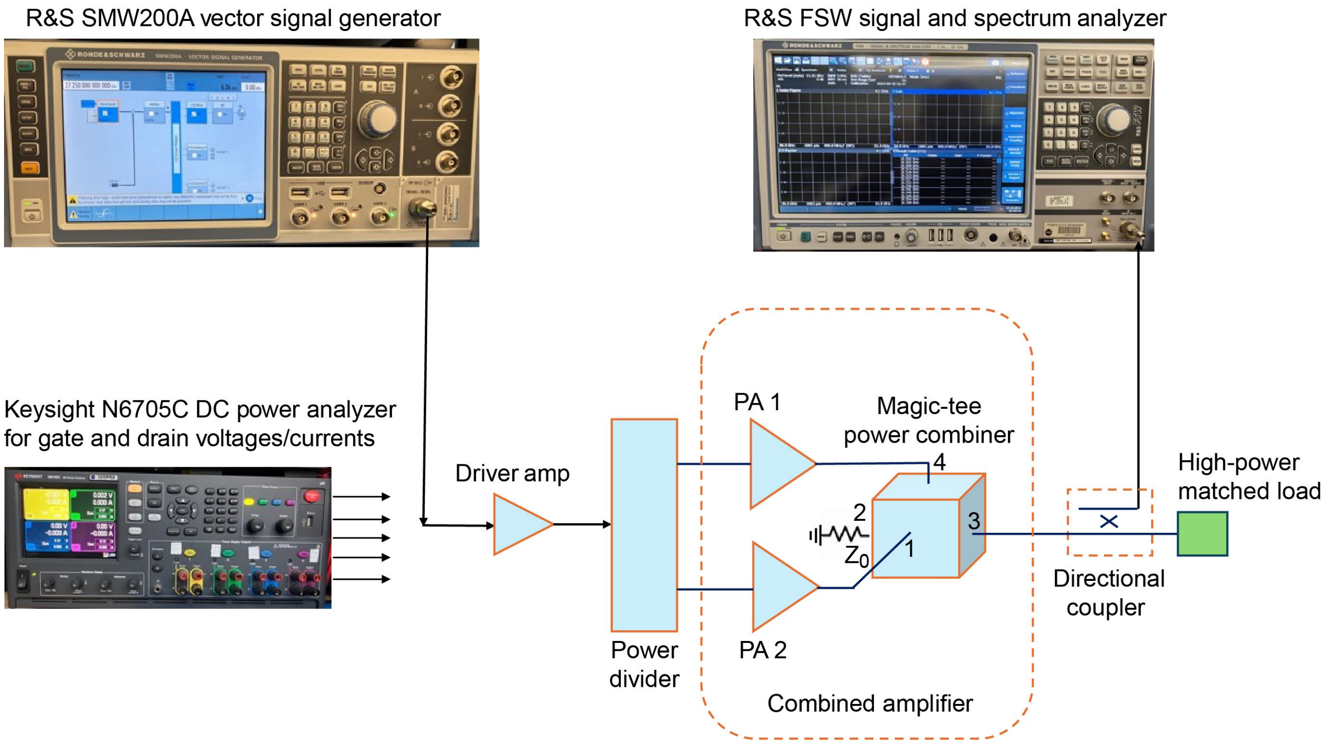

Figure 2.—Test setup for characterizing GaN HPA that uses a waveguide magic-tee as a 2-way power combiner circuit.

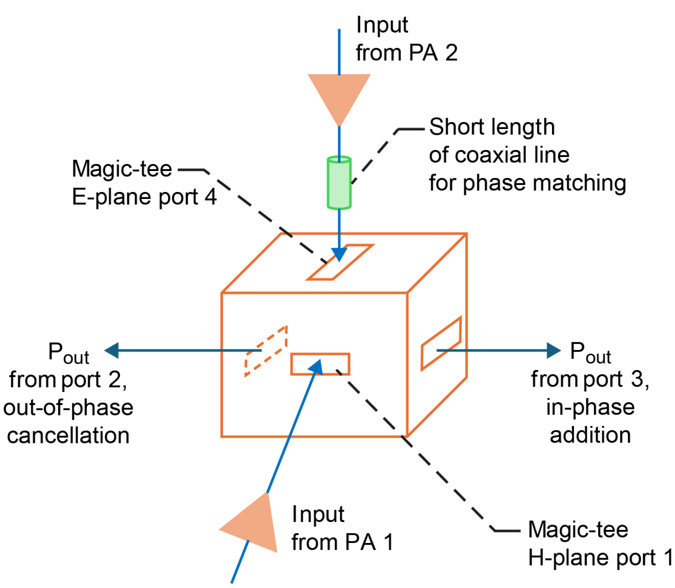

Figure 3.—Phase matching the input power to ports 1 and 4 of the magic-tee.

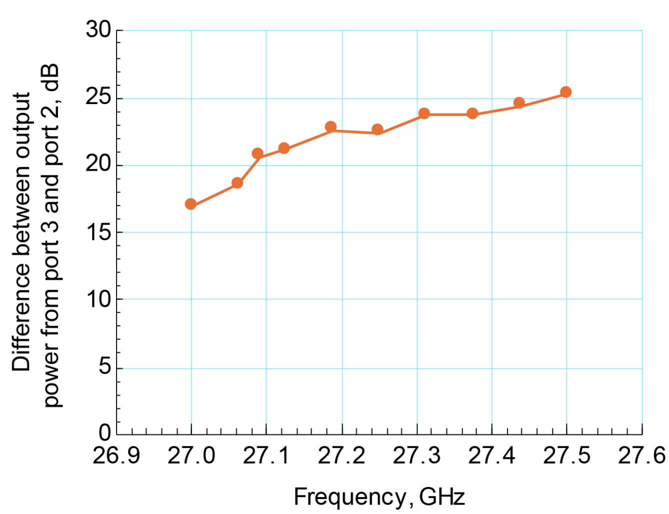

Figure 4.—Measured difference between output power from port 3 and port 2 of magic-tee.

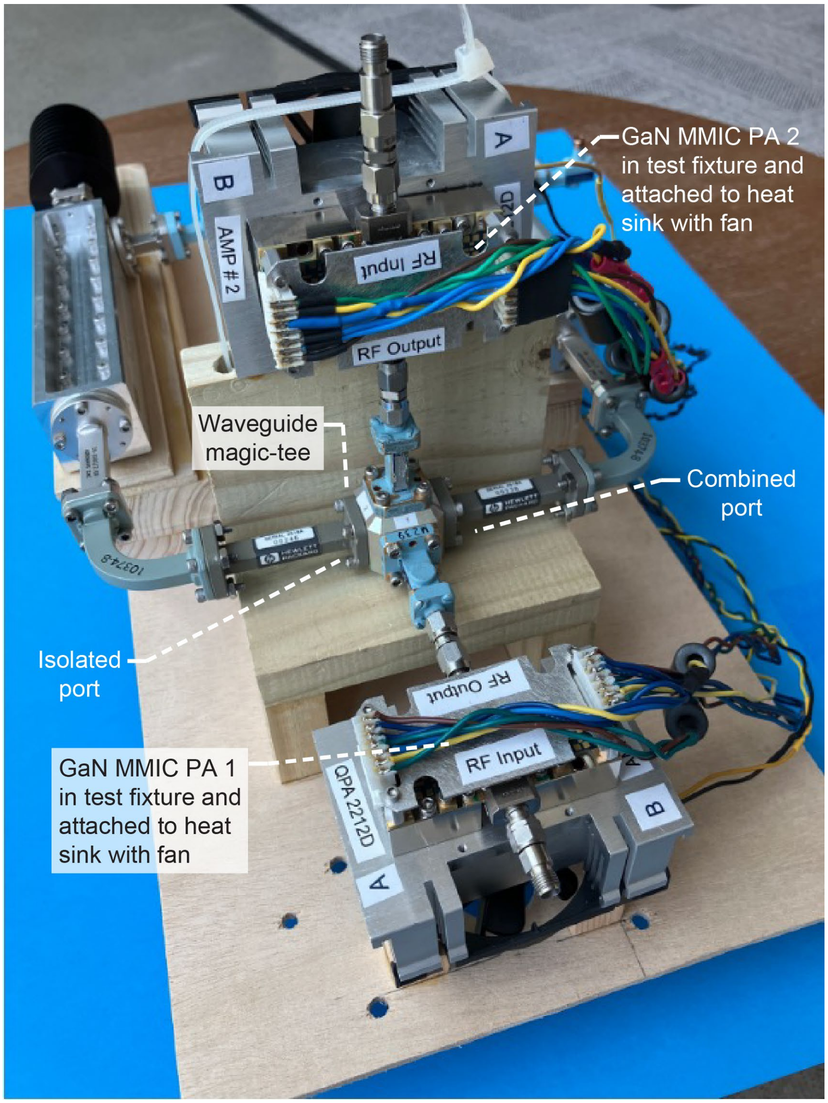

Figure 5.—A prototype HPA using a waveguide magic-tee for power combining the output from two GaN MMIC based power amplifiers.

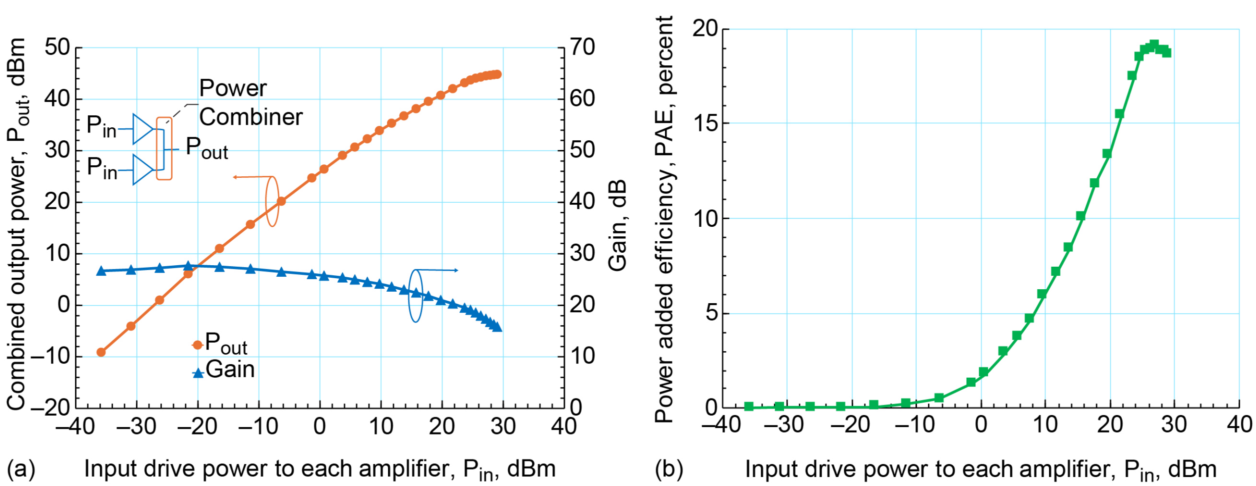

Figure 6.—(a) Measured P_{out} and gain versus P_{in} of PA with magic-tee as a 2-way power combiner at f_0 = 27.25 GHz. $V_{d1} = V_{d2}$ = 22 V, V_{g1} = –2.37 V, V_{g2} = –2.4 V. (b) Measured corresponding PAE versus P_{in}.

3.3 Error Vector Magnitude (EVM)

In the past, constant amplitude type waveforms such as Offset-QPSK was typically employed for space-to-Earth data transmission. The reason was that the PA could operate at its peak PAE when driven close to saturation and thus conserve spacecraft prime power. However, in the future there may be a desire to use spectrally efficient higher-order modulation techniques to down link data from the lunar surface/orbit. This may need HPAs with excellent linearity and PAE for signal amplification. To demonstrate this capability, the EVM at the output of the prototype HPA is measured for the Offset-QPSK, 8PSK, 16APSK, 32APSK, and 16QAM waveform constellations. The measurements are performed as a function of P_{in} at a fixed rate of 100 Msymbols/s which is typical for most applications. The measured EVM for all five waveforms at f_0 of 27.25 GHz is presented in Figure 7 and shows the change in EVM as P_{in} gradually increases from small signal to saturation. When P_{in} is backed-off by 1-dB from P_{sat}, the RMS EVM for Offset-QPSK, 8PSK, and 16APSK waveforms is small and less than 5 percent. When backed-off by 2-dB from P_{sat}, the RMS EVM for 32APSK and 16QAM waveforms are also less than 5 percent. The low RMS EVM demonstrates good linearity and enables spacecraft radio to support CCSDS as well as DVB-S2 compliant waveforms.

3.4 Waveform Constellations, Spectrum, and Spectral Regrowth

The waveform constellations are shown in Figure 8. The measured spectrum for all five waveforms at f_0 is presented in Figure 9. The results indicate that the spectral efficiency for a fixed bandwidth of 125 MHz increases from 2 to 5 bits/s/Hz. Additionally, the out-of-band spectral regrowth measured at 1-symbol rate (100 MHz) away from f_0 (that is at 27.35 GHz) for all five waveforms are indicated by a red dash line in Figure 9. The data indicates that the spectral regrowth for Offset-QPSK and 8PSK waveforms when the HPA is operated at saturation is less than 24.8 and 25.2 dBc, respectively. The spectral regrowth for 16APSK, 32APSK, and 16QAM waveforms when the HPA is backed-off from saturation by 1-dB is less than 27.5, 26.5, and 27.7 dBc, respectively. These results demonstrate low adjacent channel interference or adjacent channel power ratio (ACPR).

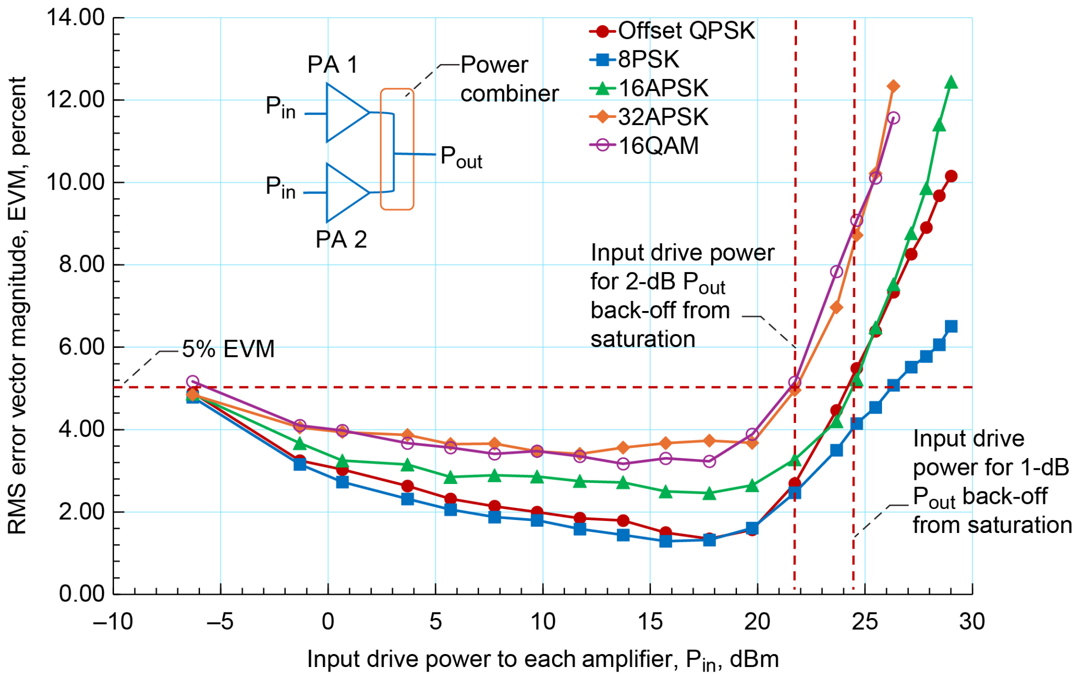

Figure 7.—Measured RMS EVM versus P_{in} at f_0 = 27.25 GHz. Symbol rate is 100 Msymbols/s and square-root raised-cosine (SRRC) filter is set to 0.35.

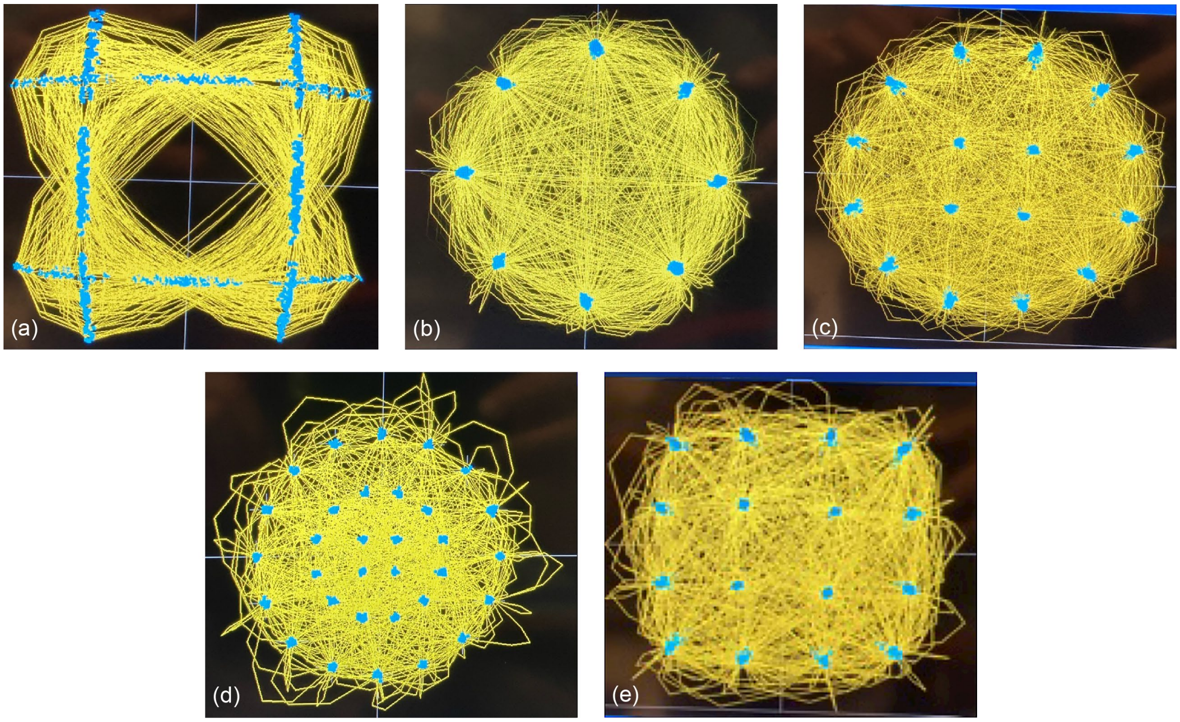

Figure 8.—Waveform constellations. (a) Offset QPSK. (b) 8PSK. (c) 16APSK. (d) 32APSK. (e) 16QAM.

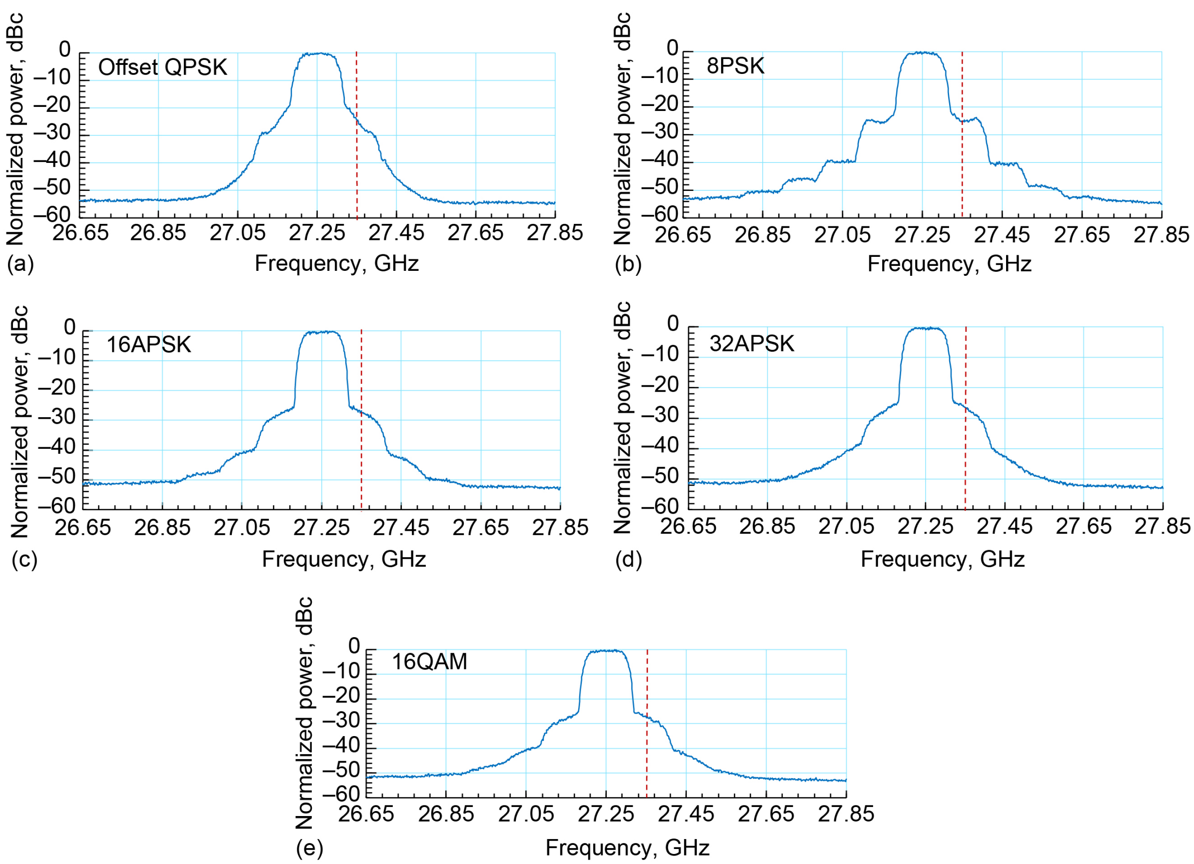

Figure 9.—Measured spectrum. Carrier frequency is 27.25 GHz, symbol rate is 100Msymbols per second, square root raised cosine (SRRC) filter is set to 0.35, and bandwidth is 125 MHz. (a) Offset QPSK. (b) 8PSK. (c) 16APSK. (d) 32APSK. (e) 16QAM.

TABLE I.—PROTOTYPE HPA PERFORMANCE SUMMARY

Parameter	Measured value
Frequency (GHz)	27 to 27.5
P_{sat} (dBm)	44.83 (30.41 W)
PAE at saturation (%)	18.7
Small signal gain (dB)	27.5
RMS EVM for Offset-QPSK, 8PSK, and 16APSK waveforms at 1-dB back-off from saturation (%)	≤ 5
RMS EVM for 32APSK and 16QAM waveforms at 2-dB back-off from saturation (%)	≤ 5
Out-of-band spectral regrowth at 27.35 GHz for Offset-QPSK and 8PSK waveforms at saturation (dBc)	< 24.8 and < 25.2, respectively
Out-of-band spectral regrowth at 27.35 GHz for 16APSK, 32APSK, and 16QAM waveforms at 1-dB back-off from saturation (dBc)	< 27.5, < 26.5, and < 27.7, respectively

4.0 Conclusions and Discussions

The architecture of a 2-way power combiner based on a waveguide hybrid magic-tee is presented. The design and brief set of specifications for a 27.0 to 27.5 GHz GaN HEMT MMIC based HPA is presented. The design is validated by characterizing a protype HPA that uses a magic-tee for 2-way power combining. The measured output power, gain, power added efficiency, error vector magnitude for Offset-QPSK, 8PSK, 16APSK, 32APSK, and 16QAM waveforms are presented. Furthermore, when the HPA is operated near saturation, the output spectrum and the out-of-band spectral regrowth for the above waveforms are also presented. The prototype HPA overall performance summary at f_0 is presented in Table I. No de-rating and no estimation of the HEMT junction temperature were performed. The above prototype HPA development is at technology readiness level of 4.

References

1. R. Giofre, L. Cabria, R. Leblanc, M. Lopez, F. Vitobello, and P. Colantonio, "An efficient and linear SSPA with embedded power flexibility for Ka-band downlink satcom applications," *IEEE Trans. Microwave Theory Tech.*, vol. 72, no. 1, pp. 563–574, Jan. 2024.
2. P. Neininger, L. John, M. Zink, D. Meder, M. Kuri, A. Tessmann, C. Friesicke, M. Mikulla, R. Quay, and T. Zwick, "Broadband 100-w Ka-band SSPA based on GaN power amplifiers," *IEEE Microwave and Wireless Components Letters*, vol. 32, no. 6, pp. 708–711, June 2022.
3. N. Estella, E. Camargo, J. Schellenberg, and L. Bui, "High-efficiency, Ka-band GaN power amplifiers," *2019 IEEE MTT-S Inter. Microwave Symposium Dig.*, Boston, MA, pp. 568–571, June 2–7, 2019.
4. E.G. Wintucky, R.N. Simons, K.R. Vaden, G.G. Lesny, and J.L. Glass, "High Power Combining of Ka-Band TWTs for Deep Space Communications," *2006 IEEE Inter. Vacuum Electronics and IEEE Inter. Vacuum Electron Sources Conference Digest (IVEC/IVESC 2006)*, pp. 63–64, Monterey, CA, April 25–27, 2006.
5. R.N. Simons, E.G. Wintucky, J.D. Wilson, and D.A. Force, "Ultra High Power and Efficiency Space TWTA Power Combiner with Reduced Size and Mass for NASA Missions," *IEEE Trans. Microwave Theory Tech.*, vol. 57, no. 3, pp. 582–588, March 2009.
6. K.R. Vaden and R.N. Simons, "Computer Aided Design of Ka-band Waveguide Power Combining Architectures for Interplanetary Spacecraft," *2005 IEEE Antennas and Propagation Society International Symposium Dig.*, pp. 635–638, Washington, D.C., July 3–8, 2005. (NASA/TM—2006-214108, Feb. 2006) (Available at https://ntrs.nasa.gov).
7. R.N. Simons, J.A. Downey, B.L. Schoenholz, M.T. Piasecki, N.T. Pham, M.K. Siddiqui, and R.G. Bonnin, "Demonstration of a Switched Wideband GaN High-Power Amplifier for Future Space Missions," *2023 IEEE Space Hardware and Radio Conference*, Las Vegas, NV, Jan. 22–25, 2023.
8. R.N. Simons, A.M. Gannon, J.A. Downey, M.T. Piasecki, and B.L. Schoenholz, "Benefits of Ka-band GaN MMIC High Power Amplifiers with Wide Bandwidth and High Spectral/Power Added Efficiencies for Cognitive Radio Platforms," *2023 IEEE Cognitive Communications for Aerospace Applications Workshop (CCAAW)*, Cleveland, OH, June 20–22, 2023.
9. R.N. Simons, M.T. Piasecki, J.A. Downey, B.L. Schoenholz, M.K. Siddiqui, "Demonstration of GaN HEMT MMIC High-Power Amplifier for Lunar Proximity Communications," *2024 IEEE Space Hardware and Radio Conference*, San Antonio, TX, Jan. 21–24, 2024.